

Molecular Dynamics Simulation of Prewetting[†]

S. Toxvaerd*

Department of Chemistry, H. C. Ørsted Institute, DK-2100 Copenhagen Ø, Denmark and DNRF Centre “Glas and Time”, Department of Science, Roskilde University, Postbox 260, DK-4000, Roskilde, Denmark

Received: May 14, 2007; In Final Form: August 16, 2007

Large-scale molecular dynamics simulations are used to determine the phase diagram of a Lennard–Jones system with and without prewetting. The simulations show that the normal condensation in the homogeneous bulk system, in the case of an attractive solid surface, is extended with a single first-order prewetting phase transition to a fluid layer of a thickness that varies from only one fluid layer for a strong attractive surface to a film of three layers of particles in the case of a weaker prewetting surface. A particle-structured surface (face-centered cubic (111)) has only marginal impact on the prewetting transition. The new triple-point temperature is significantly lower than the triple-point temperature for the bulk system.

I. Introduction

An attractive solid surface will adsorb particles. The particles might form a thin fluid film in equilibrium with a gas of the substrate particles for a vapor pressure below the vapor pressure of the coexisting bulk liquid and gas of the adsorbate. The phenomenon is named prewetting. In 1977, Cahn¹ and Ebner and Saam² independently proposed this existence of such stable prewetted films adsorbed at solid surfaces. Ebner and Saam’s solid surface is a perfect smooth wall, given by the potential

$$u_{g-3}(z) = \frac{2\pi\rho_w\sigma_w^3}{3} \epsilon_w \left[\frac{2}{15} \left(\frac{z}{\sigma_w} \right)^{-9} - \left(\frac{z}{\sigma_w} \right)^{-3} \right] \quad (1)$$

with values of the solid density ρ_w and potential parameters (ϵ_w, σ_w) for Argon adsorbed at a CO₂(s) substrate. This potential was later used as a standard substrate potential for modeling and simulations of prewetting. With this potential and for the values of $\rho_w, \epsilon_w,$ and σ_w used by Ebner and Saam, they obtain a film with a thickness corresponding to about three fluid layers of particles. The density-functional models have been refined and extended^{3–7} and supported by computer simulations^{8–15} as well as experiments.^{16–18} For a review of wetting and prewetting, see ref 19.

In the density-functional models and in computer simulations, the corresponding potential energy between particles is (self-consistently) given by Lennard–Jones (LJ) potentials. The phase diagram for the films has, however, not been determined. One of the obstacles is the determination of the precise location of the triple point for the LJ system. Especially in the molecular dynamics (MD) simulations, one typically truncates the LJ potential at a certain pair distance, r_{cut} , and the contributions from longer-ranged particle interactions $r > r_{\text{cut}}$ can easily be included as (small) mean-field corrections to the values of, for example, the pressure of bulk systems. However, these asymptotic contributions change the location of the triple point significantly as well as the location of the critical point.²⁰ The location of the triple point is determined by integrations of thermodynamic state points from, for example, an Einstein crystal and an ideal gas, respectively. But in this article, it is

demonstrated that the triple point can be determined directly and with high accuracy by MD simulations as the state with the three coexisting bulk phases in mutual equilibrium. The line of coexisting prewetted films in equilibrium with bulk gas and its connection with the phase diagram for the bulk system can also be determined directly by MD. It is possible to obtain these thermodynamic properties by “brute-force” MD because of the development of computers, which now allows one to follow systems of 10^4 – 10^5 LJ particles in up to 0.1–1 μs .

The substrate potential used by Ebner and Saam is about 35% stronger than the potential from a corresponding semi-infinite continuum of a solid of LJ particles at the triple point. In this article, it is also shown that a significantly less attractive substrate potential than that used by Ebner and Saam still gives stable prewetted films of a thickness of approximately three layers of particles. Additionally, when the strength is increased, the prewetting transition appears at a much lower gas-pressure, and the films consist of only one to two layers.

The MD systems and the computational details are given in section II, which also contains the phase diagram for the bulk LJ system. The data for prewetting is given in section III, and the discussion and conclusions are given in section IV.

II. Phase Diagram for the Bulk System

The first to obtain the phase diagram for the LJ system were Hansen and Verlet.²¹ In MD simulation, the pair-potential is usually truncated at a certain distance, and this truncation affects the locations of both the triple point and the critical point. Smit²⁰ has performed extensive Gibbs ensemble simulations for the truncated and shifted LJ potential

$$u(r) = u_{\text{LJ}}(r) = \begin{cases} 4\epsilon \left[\left(\frac{\sigma}{r} \right)^{12} - \left(\frac{\sigma}{r} \right)^6 \right] - u_{\text{LJ}}(r_{\text{cut}}), & r < r_{\text{cut}} \\ 0, & r \geq r_{\text{cut}} \end{cases} \quad (2)$$

and obtained the coexisting line(s) of liquid and gas for potential 2 for $r_{\text{cut}} = 2.5\sigma$. The location of the critical point is changed significantly by the truncation of potential 2, from $T_c = 1.316$ to $T_c = 1.085$.²⁰ The location of the triple point is also changed from $T_t = 0.68$ ²¹ to the present determination $T_t = 0.618$.

The phase diagram for coexisting bulk systems of LJ particles is determined by MD by simulating systems of $N = 40\,000$ LJ

[†] Part of the “Keith E. Gubbins Festschrift”.

* Corresponding author. E-mail: st@ruc.dk.

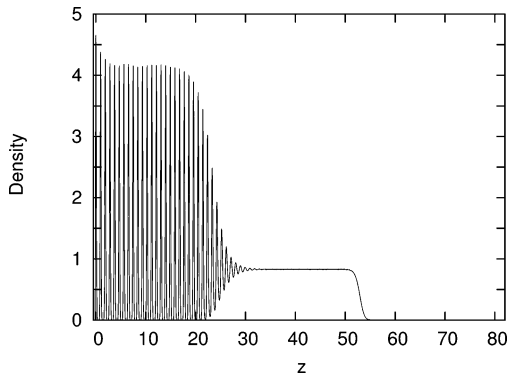


Figure 1. Density profile, $\rho(z)$, of the system of coexisting solid–liquid–gas at the triple point.

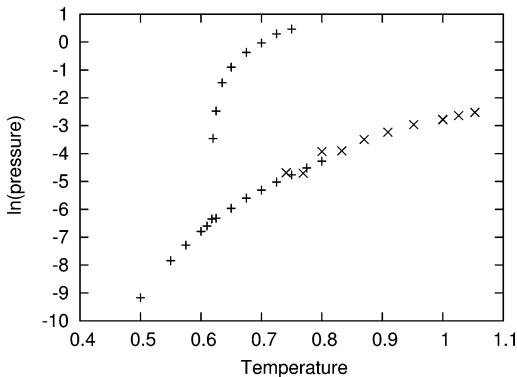


Figure 2. The pressure, $P(T)$, of coexisting phases as a function of the temperature, T . The data are shown as $\ln P(T)$. + is the present data, and \times is the data from ref 20.

particles, truncated and shifted at $r_{\text{cut}} = 2.5\sigma$ within a volume $V = l_x \times l_y \times l_z$, and $l_y = \sqrt{3}/2 \times l_x$, where $l_x = n \times d$. The lattice constant, d , was equal to the minimum in the LJ potential, $r_0 = 2^{1/6}\sigma$, in most of the simulations.²² There are periodic boundaries in the x and y directions. In the z direction, the N particles are confined between $z = 0$ and $z = l_z$ (in most of the simulations). The choice of l_x and l_y ensures that the system can freeze into a solid with face-centered cubic (fcc) or hexagonal close-packed (hcp) lattice structure, and with the (111) plane in the (x,y) direction. The pressure is determined as the normal component, P_n of the pressure tensor.²³ All the MD systems are calibrated at a certain temperature and volume, and equilibrium is observed typically after $\sim 30\text{--}50$ ns (3×10^6 to 5×10^6 time steps).²⁴

Equilibrium between coexisting bulk phases is determined as the state where the planar interfaces (in the x,y planes) do not move, but are stationary. Starting at low temperatures with a solid in equilibrium with the gas, one observes that the solid by heating begins to melt at a certain temperature, and it is possible to locate this (triple-point) temperature with high precision. Figure 1 shows the density profile, $\rho(z)$, of coexisting solid–liquid–gas at the triple point ($P_t = 0.00162$, $T_t = 0.618$), obtained after the equilibration, from the next 10^6 time steps (~ 10 ns). The densities of the three phases are $\rho(s) = 0.9333$, $\rho(l) = 0.8290$, and $\rho(g) = 0.00262$. If the temperature is changed by ± 0.001 , the solid–liquid interface, at $\approx 25\sigma$, moves to the left or right, respectively, with a few σ within the next 10 ns. The phase diagrams are shown in Figures 2 and 3. There is good agreement with Smit’s Gibbs-ensemble data for the same (but much smaller) system, as can be seen from the figures.

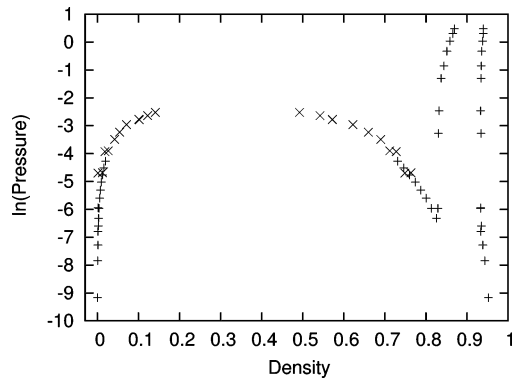


Figure 3. The $\ln P(\rho)$ phase diagram. + is the present data, and \times is the data from ref 20.

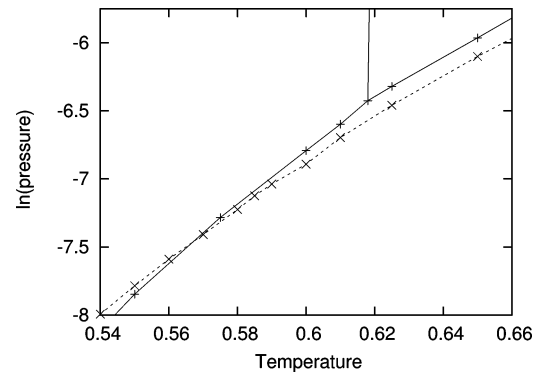


Figure 4. The $\ln P(T)$ phase diagram in the vicinity of the triple-points. The phase diagram for the bulk LJ system is shown with + and a solid line, and the coexisting line, $\ln P_{\text{pw-g}}(T)$, between the prewetted film and the bulk gas is shown with \times and a dashed line.

III. Prewetted Films

The substrate potential used by Ebner and Saam is about 35% stronger than the potential from a corresponding semi-infinite continuum of a solid of LJ particles at the triple point. It is intuitively understandable that condensation might give a prewetted film when the attraction of the adsorbing substrate is sufficiently strong. However, it raises the question of how strong the substrate attraction needs to be in order to ensure prewetting, what happens when the interaction is further increased, and to what extent a lattice structure of the surface of the substrate affects the establishment of the prewetted film.

The investigation of prewetting was started by a determination of the coexisting line, $P_{\text{pw-g}}(T)$, of prewetted film in equilibrium with bulk gas and for potential 1. The prewetted films were obtained in MD systems with $N = 20\,000$ LJ particles. Prewetting is a first-order phase transition.¹³ If the pressure is decreased (by length-scaling in the x,y directions) the film breaks, but the pressure remains constant during this first-order prewetting transition (for determination of the pressure, P_n , of coexisting prewetted film and gas, see later text). The first-order phase transition is associated with hysteresis, and it is, for example, possible to cool the fluid film down to a temperature below the evaporation temperature of bulk solid adsorbate. Figure 4 shows the details of the combined phase diagram in the vicinity of the two triple-points. The triple point between bulk solid, prewetted fluid film, and gas is $T_t(\text{pw}) = 0.57$ and $P_t(\text{pw}) = 0.000628$, and it means that a prewetted solid surface can be covered by a fluid film below the (bulk) triple-point temperature for the adsorbate.

If the phase diagram in Figure 4 is correct, a supercooled fluid film, at a temperature below the triple-point temperature

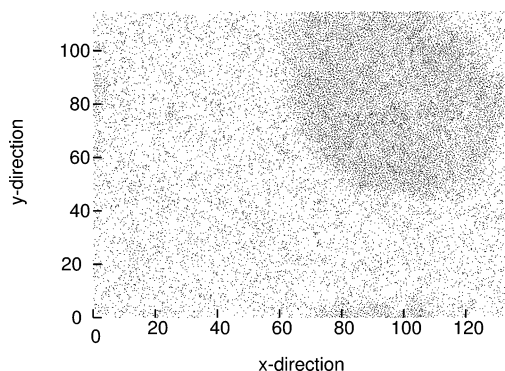


Figure 5. Top view of the fluid droplet at the start of freezing. (Periodical boundaries are in the x and y directions.)

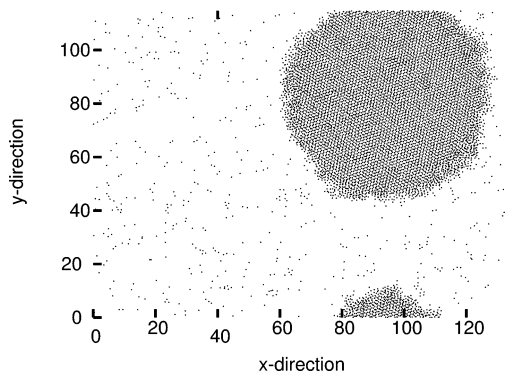


Figure 6. Top view of the droplet after freezing at $T = 0.55$.

$T_i(\text{pw})$, freezes spontaneously to a crystal with a minimum surface, so the thin film should break up and form a crystal at the surface. There is, however, a rather strong hysteresis in the supercooled film. Two sets of MD experiments were performed in order to investigate the freezing of the prewetted film.

In the first experiment, the nonequilibrium film at $T = 0.55$ (the second \times in Figure 4, obtained after 5×10^6 time steps), below the new triple-point temperature $T_i(\text{pw})$, was simulated in 6×10^7 time steps ($\sim 0.6 \mu\text{s}$). The three layers in the film of adsorbate froze during the long simulation, but without breaking up. The structure of the frozen film, however, contained many defects, and the annihilation of these defects was very slow. The pressure remained above the pressure of bulk solid adsorbate, and an analysis of the structure within the three pseudo two-dimensional (2D) adsorbed layers revealed that the layers were frozen fcc (or hcp) (111) layers with many defects and not 2D layers.^{25,26}

In the second experiment, a prewetted droplet of $\sim 20\,000$ adsorbate particles was cooled to $T = 0.55$ and followed 6×10^7 time steps. It is apparently more easy to freeze a droplet of the prewetted film. The droplet froze and formed a rather perfect hcp structure, but after 2.5×10^7 time steps ($\sim 0.25 \mu\text{s}$). The frozen droplet was followed in the next 3.5×10^7 time steps. The crystal grew slowly in the z direction and into a more compact three-dimensional (3D) form with an extension in the z direction of approximately six layers. Figures 5–7 give some details of the freezing of the droplet of a prewetted adsorbate into a 3D hcp crystal. (In other similar experiments, some of the droplets also froze into fcc order, as one should expect). Figure 5 shows a top view of the droplet at $T = 0.65$ and just before it was cooled to $T = 0.55$, and Figure 6 is correspondingly a top view of the droplet after $0.25 \mu\text{s}$. Figure 7 shows the (x,y) positions of the particles in the first and third layers and in the interval $[80\sigma, 100\sigma]$ inside the droplet. The almost

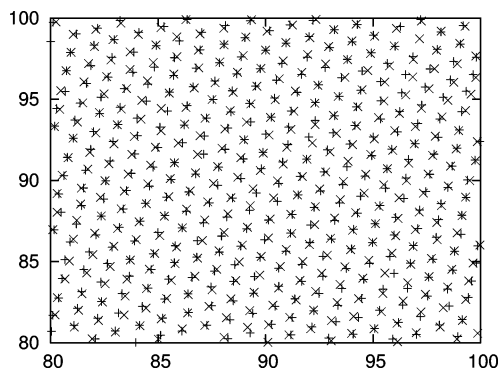


Figure 7. (x,y) positions of particles in the first and third frozen layers, and inside the droplet. The (x,y) positions of particles in the first layer are shown with $+$, and the positions in the third layer are shown with \times . The identical lattice positions show an hcp (111) structure.

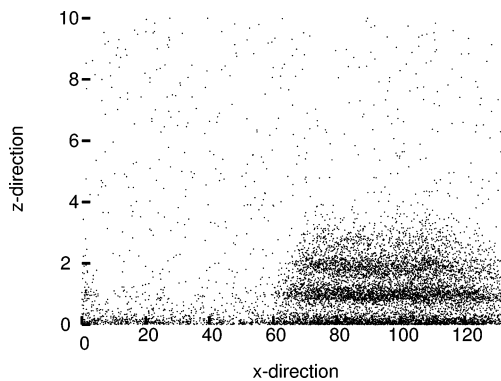


Figure 8. Side view of a fluid droplet at $T = 0.65$ (the top view is shown in Figure 5).

identical (x,y) positions of the particles in the two layers show that the fluid is frozen to a crystal with hcp order. The frozen droplet was heated to a temperature of $T = 0.59$, where it melted and formed a prewetted fluid droplet, and with a pressure equal to the pressure of the coexisting prewetted film and gas, in accordance with the phase diagram in Figure 4.

The surface force from the solid substrate on the adsorbed particles varies for different solid substrate/adsorbate systems.²⁷ As mentioned previously, the parameters $\rho_w \sigma_w^3 = 0.988$, $\sigma_w = 3.727 \text{ \AA}$, and $\epsilon_w/k_B = 153 \text{ K}$, used by ref 2 for Ar adsorbed on a $\text{CO}_2(\text{s})$ surface are a factor of 1.35 stronger than the corresponding (minimum) energy between an Ar atom and an Ar(s) surface, given by the LJ potential. With these parameter values for the potential, one obtains a transition to a prewetted film of approximately three layers. The fact that it is three layers is, for example, seen by inspection of the droplets at the transition, which shows that the particles in the first three layers are located at the (x,y) position of the droplet (Figures 5 and 8), although there is a corona of particles above the third layer. The thin droplet shown in Figure 8 of the adsorbate has a thickness of only $\sim 2\sigma$ and consists of three layers of particles with a droplet diameter of $\sim 60\sigma - 70\sigma$.

The substrate potential is still sufficient to give prewetting for an attraction in potential 1, reduced by a factor of 0.90 (corresponding to $\sim 22\%$ stronger attraction than the attraction from Ar(s)) and to a film of three layers of particles, but the surface does not prewet for weaker attractions. If one instead increases the strength of attraction, however, it has a strong impact on the appearance of prewetting. The prewetting takes place at a significantly lower pressure when the attraction is increased by a factor of only 1.1 (Figure 9), and inspection of the film and droplets shows that the droplets and film only

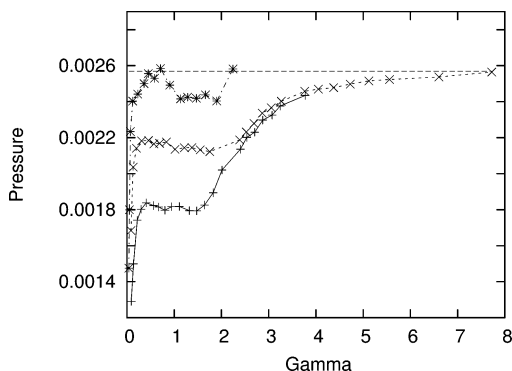


Figure 9. Pressure, P_n as a function of adsorption, Γ , for $T = 0.65$. The adsorption for the substrate potential (1) is shown with \times and dashes. The $*$ and dot-dashed line represent a reduced attraction, $0.9\epsilon_w$, and the $+$ and solid line represent $1.1\epsilon_w$ attraction. The straight line is the pressure of coexisting (bulk) liquid and gas.

consist of approximately two layers (see later text). The droplets and the prewetted film consist of only one layer for an enhanced strength of substrate (for a factor of 1.25).

Potential 1 is an idealization of a real solid substrate potential, where the effect of the atomic structure of the solid surface is ignored, so the potential is only a function of the distance to the ideal planar surface. However, the particle structure of the surface of the substrate affects the establishment of the prewetted film. It is difficult to determine a general and qualitative law for this effect.²⁸ The influence of the atomic structure of the surface was investigated by replacing the smooth substrate by a (static) fcc (111) layer of repulsive LJ particles at the surface. This layer has, however, only a marginal effect on the prewetted film and the location of the phase transition.

Condensation is a first-order phase transition, characterized by a change in density from gas to (bulk) liquid at constant pressure/chemical potential. Prewetting is correspondingly characterized by a constant (normal) pressure at increasing adsorption, Γ . The adsorption at the substrate surface is obtained from the density $\rho(z)$ as

$$\Gamma = \int_0^{l_z} [\rho(z) - \rho(g)] dz \quad (3)$$

where $\rho(g)$ is the density of the particles in the (bulk) gas. Density-functional investigations³ indicate that the adsorbate might perform a sequence of layering transitions at low temperatures. This corresponds to a much more complex phase diagram than that given by Figure 4, and the Gibbs-ensemble simulations¹¹ do not rule out this possibility. In order to investigate whether the observed prewetting is the only transition, the adsorption was determined for different pressures, P_n , and for different strengths of the substrate attraction. The values were obtained by rescaling the system in the (x,y) directions and equilibration, as described in section II. Figure 9 shows the pressure as a function of Γ for $T = 0.65$. The pressures for small droplets adsorbed at the solid surface are higher than the pressure at the prewetting film–gas transition. These excess pressures in the droplets are given by the Laplace equation. The pressure, P_n , tends toward a constant value (the plateaus in Figure 9) for increasing coverage of the $l_x \times l_y$ area with prewetted film, and the pressures of coexisting film and gas, shown in Figure 4, are determined as the pressures of these plateaus. The adsorption isotherms show that there is only one transition at this temperature, and it is to a film of a thickness of a few layers. For the strength of attraction introduced by

Ebner and Sam, the film consists of approximately three layers, which turns out to be a maximum thickness for prewetting. The transition appears at a much lower pressure and with a transition into a film of a few layers when the strength of attraction is increased; for an attraction of $1.1\epsilon_w$, it transitions into two layers (and for $1.25\epsilon_w$, it transitions into only one layer). As the pressure/density of the gas is increased, the thickness of the film grows monotonically and rapidly toward infinity as the pressure approaches the pressure of the coexisting bulk liquid and gas (dashed line in Figure 9). A sequence of layering transitions might, however, appear at lower temperatures or for longer ranges of surface attraction than given by eq 1.

IV. Discussion

A series of models with different “confined geometries” (CGs) have appeared in recent years, and simulations have revealed a richness of phase changes and complex phase behavior (see, e.g., refs 29–32 and the references therein). Capillary phenomena cover all kinds of effects from CG, and a planar smooth solid surface is the most simple example of a CG.

The existence of a fluid (film) phase at a vapor pressure well below the pressure of coexisting bulk liquid and gas has been known for many years. The adsorption isotherm of, for example, Ar and other simple molecules adsorbed on (exfoliated) graphite have a richness of phase transitions,^{32,33} but the present simulations show that a perfect planar solid surface only gives a single transition. The thickness of the prewetted film varies from a single layer of adsorbed particles to a film with a thickness corresponding to three fluid layers of particles. The thickness of the prewetted film depends on the strength of the attraction, and prewetting appears only for attraction on a gas particle that is at least 20% stronger than the attraction from a condensed phase of the adsorbate itself. In this case, the prewetted film consists of three fluid layers. For significantly stronger substrate attraction, the phase transition is into a film of only one to two layers of particles. The phase diagram (Figure 4) for prewetting shows the existing of prewetted film below the triple point for the adsorbate, and, when these films freeze, it is into 3D solids. When the prewetted film is exposed to a higher pressure than the pressure of the coexisting prewetted film and bulk gas, the thickness of the film increases monotonically and rapidly toward infinity, as the pressure approaches the pressure of the coexisting bulk liquid and gas of the adsorbate.

The present investigation at $T = 0.65$ shows no sign of a stepwise building up of the adsorbate after the establishment of the prewetted film, in contrast with theoretical models and experiments.^{3,33} The reason for this difference might be that the temperature, $T = 0.65$ is too high or that the solid substrate potential (eq 1) is too drastic a reduction of the pair interaction between an adsorbate particle and a semi-infinite solid. It could also be because exfoliated graphite consists of stacked (0001) solid planes and a much more complex CG.

References and Notes

- (1) Cahn, J. W. *J. Chem. Phys.* **1977**, *66*, 3667.
- (2) Ebner, C.; Saam, W. F. *Phys. Rev. Lett.* **1977**, *38*, 1486.
- (3) Ball, P. C.; Evans, R. *J. Chem. Phys.* **1988**, *89*, 4412.
- (4) Velasco, E.; Tarazona, P. *Phys. Rev. A* **1990**, *42*, 2454.
- (5) Sweatman, M. B. *Phys. Rev. E* **2001**, *65*, 011102.
- (6) Omata, K. *J. Non-Cryst. Solids* **2002**, *312*, 481.
- (7) Reister, E.; Müller, M.; Kumar, S. K. *Macromolecules* **2005**, *38*, 5158.
- (8) Finn, J. E.; Monson, P. A. *Phys. Rev. A* **1989**, *39*, 6402.

- (9) Finn, J. E.; Monson, P. A. *Phys. Rev. A* **1990**, *42*, 2458.
- (10) Nijmeijer, M. J. P.; Bruin, C.; Bakker, A. F.; Van Leeuwen, J. M. *J. Mol. Phys.* **1991**, *72*, 927.
- (11) Fan, Y.; Monson, P. A. *J. Chem. Phys.* **1993**, *99*, 6897.
- (12) Bojan, M. J.; Stan, G.; Curtarolo, S.; Steele, W. A.; Cole, M. W. *Phys. Rev. E* **1999**, *59*, 864.
- (13) Toxvaerd, S. *J. Chem. Phys.* **2002**, *117*, 10303.
- (14) Curtarolo, S.; Cole, M. W.; Diehl, R. D. *Phys. Rev. B* **2004**, *70*, 115403.
- (15) Errington, J. R. *Langmuir* **2004**, *20*, 3798.
- (16) Chandavarkar, S.; Geertman, R. M.; de Jeu, W. H. *Phys. Rev. Lett.* **1992**, *69*, 2384.
- (17) Luo, J.; Chiang, Y.-M. *Acta Mater.* **2000**, *48*, 4501.
- (18) Ohmasa, Y.; Kajihara, Y.; Yao, M. *Phys. Rev. E* **2001**, *63*, 051601.
- (19) Bonn, D.; Ross, D. *Rep. Prog. Phys.* **2001**, *64*, 1085.
- (20) Smit, B. *J. Chem. Phys.* **1992**, *96*, 8639. Smit, B., Ph.D. Thesis, Rijksuniversiteit Utrecht, The Netherlands, 1990.
- (21) Hansen, J.-P.; Verlet, L. *Phys. Rev.* **1969**, *184*, 151.
- (22) The lattice constant, d , is almost equal to the minimum distance r_0 in the LJ potential at low pressures, where the components, p_{xx} and p_{yy} of the pressure tensor are equal. A small adjustment ($\sim 3\%$) was performed for coexisting solid and liquid (the solid–liquid line in Figure 2) in order to ensure $p_{xx} = p_{yy}$.
- (23) Toxvaerd, S. *J. Chem. Phys.* **1981**, *74*, 1998.
- (24) For MD details, see Toxvaerd, S. *Mol. Phys.* **1991**, *72*, 159. Temperature is in units of ϵ/k , and the length is in units of σ .
- (25) Barker, J. A.; Henderson, D.; Abraham, F. F. *Physica* **1981**, *106A*, 226.
- (26) Toxvaerd, S. *Phys. Rev. A* **1981**, *24*, 2735.
- (27) Israelachvili, J. *Intermolecular & Surface Forces*; Academic Press: London, 1992.
- (28) Voronov, R. S.; Papavassiliou, D. V.; Lee, L. L. *J. Chem. Phys.* **2004**, *124*, 204701.
- (29) Coasne, B.; Hung, F. R.; Pellenq, R. J.-M.; Siperstein, F. R.; Gubbins, K. E. *Langmuir* **2006**, *22*, 194.
- (30) Striolo, A.; Chialvo, A. A.; Cummings, P. T.; Gubbins, K. E. *J. Chem. Phys.* **2006**, *124*, 074710.
- (31) Coasne, B.; Jain, S. K.; Gubbins, K. E. *Phys. Rev. Lett.* **2006**, *97*, 105702.
- (32) Thomy, A.; Duval, X. *J. Chim. Phys.* **1970**, *67*, 1101.
- (33) Thomy, A.; Duval, X. *Surf. Sci.* **1994**, *299*, 415 and references therein.